International Journal of Hydrogen Energy 177 (2025) 151653

Contents lists available at ScienceDirect

International Journal of Hydrogen Energy

journal homepage: www.elsevier.com/locate/he

Investigation of K_2TiH_6 and Ca_2TiH_6 under pressures from 0 to 20 GPa: Structural, electronic, thermodynamic, mechanical, vibrational, and hydrogen storage properties

Salih Ermiş [a], Ahmet İyigör [b], Cihan Kürkçü [c,*]

[a] Department of Electrical and Electronic Engineering, Kırşehir Ahi Evran University, Kırşehir, Türkiye
[b] Department of Machine and Metal Technologies, Kırşehir Ahi Evran University, Kırşehir, Türkiye
[c] Department of Electronics and Automation, Kırşehir Ahi Evran University, Kırşehir, Türkiye

ARTICLE INFO

Handling editor: M Mahdi Najafpour

Keywords:
X_2TiH_6
Hydrogen storage
First-principles calculations
Mechanical properties
Thermodynamic stability

ABSTRACT

In the face of the global energy crisis and increasing environmental pollution, the demand for sustainable and clean energy systems has accelerated research on hydrogen as a promising energy carrier due to its high energy density and zero-carbon emissions. However, efficient and safe storage remains a major technological challenge. In this study, the structural, electronic, elastic, thermodynamic, phonon, and hydrogen storage properties of K_2TiH_6 and Ca_2TiH_6 complex hydride compounds were systematically investigated in the 0–20 GPa pressure range using first-principles calculations based on density functional theory (DFT). Electronic band structure analyses revealed that the K_2TiH_6 compound exhibits a non-magnetic semiconducting character, while the Ca_2TiH_6 compound demonstrates ferromagnetic properties and exhibits metallic behavior. The evaluation of elastic properties revealed that both compounds meet mechanical stability criteria. Based on B/G and Poisson's ratio values, K_2TiH_6 exhibits brittle behavior at 0 GPa pressure but gains ductile properties at all other pressure values. Ca_2TiH_6, on the other hand, exhibits ductile behavior in the 0–20 GPa range. Vibrational and thermodynamic analyses revealed that an increase in temperature results in an increase in vibrational energy and entropy. Conversely, under high pressure, there is an increase in structural rigidity and a decrease in atomic disorder. It was determined that the Ca_2TiH_6 compound exhibits superior rigidity and ductility properties from room conditions onward. As a result of the phonon calculation, both compounds are dynamically stable. Importantly, hydrogen storage evaluations indicated gravimetric capacities of 4.58 wt% for K_2TiH_6 and 4.51 wt % for Ca_2TiH_6, with desorption temperatures of 55 K and 274 K, respectively, suggesting their suitability for low- and moderate-temperature hydrogen release applications. These findings provide valuable insights into the pressure-dependent stability and storage potential of complex hydrides, highlighting K_2TiH_6 and Ca_2TiH_6 as promising candidates for next-generation hydrogen energy systems.

1. Introduction

The increasing global demand for clean and sustainable energy systems, hydrogen has gained significant attention due to its high energy density and environmentally friendly characteristics. However, the safe, efficient, and practical storage of hydrogen remains a major technological challenge, necessitating the exploration of advanced materials capable of reversible hydrogen uptake and release under moderate conditions [1,2]. In today's world, where energy demand is constantly increasing, the need for environmentally friendly, sustainable, and highly efficient energy systems has accelerated research into alternative energy sources [3,4]. Hydrogen energy stands out as the energy carrier of the future due to its low environmental impact and high energy density. However, the effective and safe storage of hydrogen remains one of the key technical challenges hindering the widespread adoption of this energy system [5–8]. The low density of hydrogen in its gaseous phase limits its volumetric efficiency for storage. For this reason, storing hydrogen in solid materials such as metal hydrides is considered a safer and more portable alternative. Complex metal hydrides attract attention due to their high hydrogen capacity, reversible adsorption-desorption processes, and stable structures under certain conditions [9,10].

The K_2TiH_6 and Ca_2TiH_6 compounds were selected considering the

* Corresponding author.
E-mail addresses: sermis@ahievran.edu.tr (S. Ermiş), ahmetiyigor@ahievran.edu.tr (A. İyigör), ckurkcu@ahievran.edu.tr (C. Kürkçü).

https://doi.org/10.1016/j.ijhydene.2025.151653
Received 7 July 2025; Received in revised form 8 September 2025; Accepted 18 September 2025
Available online 22 September 2025

stability and hydrogen storage capacities of similar Ti-based complex hydrides that have already been synthesized and investigated experimentally [11]. These compounds crystallize in a cubic $Fm\bar{3}m$ structure composed of $[TiH_6]^{2-}$ octahedral units, which ensures high hydrogen density and structural stability. Our calculations further revealed that both compounds possess gravimetric hydrogen storage capacities of about 4.5 wt% and exhibit different desorption temperatures, making them practical candidates for low- and medium-temperature applications. Although experimental studies in the literature have demonstrated the promise of related alkali and alkaline-earth Ti-hydrides for hydrogen storage [12], no comprehensive first-principles investigation has been carried out on K_2TiH_6 and Ca_2TiH_6 under high-pressure conditions. Therefore, the selected compounds are both experimentally grounded and practically relevant, while also representing novel material candidates for hydrogen storage. Recent studies have shown that complex hydrides formed by alkali and alkaline earth metals with titanium exhibit interesting physical properties, particularly under high pressure, by transitioning to new electronic and structural phases [12,13]. The compounds K_2TiH_6 and Ca_2TiH_6 have become of interest not only for their hydrogen storage potential but also for their stability under high pressure, structural phase transitions, electronic structure changes, and thermophysical behavior. Hydrostatic pressure strongly influences material properties by reducing interatomic distances and modifying orbital overlaps. This results in systematic decreases in lattice parameters and cell volume, leading to higher density and enhanced structural stability. The strengthening of interatomic interactions under pressure lowers the formation enthalpy, thereby stabilizing the hydride framework. Pressure also alters the electronic band structure: increased orbital overlap near the Fermi level can shift or modify band gaps, directly affecting conductivity and optical responses such as dielectric function, absorption, and reflectivity. Thus, pressure serves as a powerful external parameter to tune both the structural and functional properties of hydrides, providing insights into their hydrogen storage performance under varying conditions. Studies conducted on similar compounds in the literature have revealed that such structures may exhibit special phases such as metal–insulator transitions, magnetic property changes, or superconductivity under high pressure [11,14]. Complex metal hydrides, particularly those involving alkali and alkaline earth metals with transition metals, have emerged as promising candidates due to their high gravimetric storage capacity and stability under certain pressure and temperature conditions. Understanding the structural, mechanical, electronic, and thermodynamic properties of such hydrides under varying pressures is critical for designing efficient hydrogen storage systems and for gaining insights into their potential integration into next-generation clean energy technologies. Furthermore, the results obtained in this study indicate that the K_2TiH_6 and Ca_2TiH_6 compounds examined under pressure exhibit stable structures. The literature contains studies that monitor the damage and brittleness caused by hydrogen in steel structures using ultrasonic methods [15], highlighting the critical role of hydrogen in different material systems. In recent years, advanced data processing and imaging methods have enabled more accurate analysis of the structural and functional properties of materials. For example, combining thermographic measurements with signal processing techniques enables the precise examination of the thermal and mechanical behavior of complex materials [16]. Such approaches also serve as a guide in the multidimensional analysis of new-generation energy compounds, such as hydrogen storage materials.

The present study aims to comprehensively investigate the structural, electronic, mechanical, thermodynamic, vibrational, and hydrogen storage properties of X_2TiH_6 (X = K, Ca) hydrides within the 0–20 GPa pressure range by means of density functional theory calculations. These pressures were chosen to systematically study trends. While industrial systems often operate below 5 GPa, our range allows extrapolation and provides insight into high-pressure stability relevant for hydrogen storage research. 0 GPa only indicates normal conditions; systematic analysis under different pressures is required to understand hydrogen storage properties. This allows us to understand how materials will behave in real storage environments and how their stability and capacity will change. Additionally, in real hydrogen storage environments, materials do not operate solely at atmospheric pressure (0 GPa). Tanks, cells, and solid-state storage environments are exposed to different pressure conditions. Therefore, it is necessary to understand how materials behave not only at 0 GPa but also under high-pressure conditions. This systematic approach allows us to establish clear correlations between bonding nature, stability, and hydrogen release behavior under pressure. The most attractive outcome of our research is related to the hydrogen storage performance: K_2TiH_6 exhibits a gravimetric capacity of 4.58 wt% with a remarkably low desorption temperature of 55 K, while Ca_2TiH_6 provides a capacity of 4.51 wt% and a moderate desorption temperature of 274 K. These results suggest that K_2TiH_6 is a promising candidate for low-temperature hydrogen release applications, whereas Ca_2TiH_6 offers superior structural rigidity and ductility, making it more suitable for hydrogen release at moderate operating conditions. By combining high storage capacity, structural stability under pressure, and tunable desorption temperatures, X_2TiH_6 hydrides emerge as promising candidates for next-generation hydrogen-based clean energy technologies.

2. Calculation methods

In this study, the structural, electronic, elastic, thermodynamic, vibrational, and hydrogen storage properties of K_2TiH_6 and Ca_2TiH_6 were systematically investigated using density functional theory (DFT) within the generalized gradient approximation (GGA) of Perdew–Burke–Ernzerhof (PBE) [17], to evaluate their potential for hydrogen storage. All calculations were performed using the plane wave-based Quantum ESPRESSO [18,19] software package. For electron-ion interactions, both norm-conserving and ultrasoft potentials were preferred. Appropriate energy cutoff values were selected for valence electrons based on plane waves, and all calculations converged at these energy values.

To determine the structural properties, volume optimization was performed for each compound, and the most suitable volume values corresponding to the total energy were found. In the geometry optimizations, the forces were kept below 10^{-7} Ry/Bohr, and the pressure was kept below 0.5 kbar to obtain the equilibrium states of the structures. A 12x12x12 Monkhorst-Pack [20] k-point grid was used for Brillouin zone sampling, and an appropriate k-point grid was selected for all calculations to ensure energy convergence. Electronic structure calculations were performed on optimized structures. Band structures were calculated along high-symmetry directions, and band gaps were determined. Additionally, total and atomic partial density of states (DOS) calculations were performed, and the conductivity types and atomic contributions of the compounds were analyzed. In these calculations, a dense 24x24x24 k-point grid was used to achieve a more precise energy resolution. Convergence tests were performed by increasing the k-point density systematically (from $6 \times 6 \times 6$ up to $24 \times 24 \times 24$). The total energy and electronic density of states were monitored. We confirmed convergence when changes in total energy were less than 1 meV/atom. Hence, a $12 \times 12 \times 12$ grid was selected for geometry optimization and a denser $24 \times 24 \times 24$ grid for DOS calculations.

Elastic constants were calculated using the Thermo-pw [21] program with structures optimized at each pressure point to determine mechanical (elastic) properties. Calculations were performed at pressure values of 0, 5, 10, 15, and 20 GPa. For each pressure value, elastic constants were obtained through stress-strain relationships formed by applying small deformations consistent with symmetry. Parameters such as bulk modulus (B), shear modulus (G), Young's modulus (E), Poisson's ratio (ν), and Pugh ratio (B/G) were calculated using these constants. Additionally, thermodynamic properties were derived from the elastic

constants using the Thermo-pw module. Each pressure and other related thermodynamic quantities were calculated. Thus, the pressure resistance and application potential of the compounds were evaluated.

3. Results and discussions

3.1. Structural properties

The physical properties of X_2TiH_6 (X = K, and Ca) compound under different hydrostatic pressure values (0, 5, 10, 15, and 20 GPa) were calculated using the density functional theory with the Quantum ESPRESSO package program. Under ambient conditions, K_2TiH_6 and Ca_2TiH_6 crystallize in a cubic structure with space group $Fm\bar{3}m$ (Space Group No: 225). Each unit cell of these compounds contains 9 atoms. The lattice constant values of the K_2TiH_6 compound are a = b = c = 8.5535 Å, and the angles are $\alpha = \beta = \gamma = 90^\circ$. The lattice constant values of the Ca_2TiH_6 compound are a = b = c = 7.4698 Å, and the angles are $\alpha = \beta = \gamma = 90^\circ$. A view of the crystal structure of the X_2TiH_6 compound obtained from different directions is shown in Fig. 1. The lattice parameter, volume, and density values calculated at pressure values of 0, 5, 10, 15, and 20 GPa are given in Table 1.

The formation energy, a critical parameter for hydrogen storage materials, is derived from Equation (1) [22].

$$\Delta H_f = E_{tot}(X_2TiH_6) - E_{tot}(X_2) - E_{tot}(Ti) - 3E_{tot}(H_2) \quad (1)$$

In equation (1), the total energies of the compounds $E_{tot}(X_2TiH_6)$, $E_{tot}(X_2)$, $E_{tot}(Ti)$, and $E_{tot}(H_2)$ denote the total energies of X (K and Ca), Ti, and H_2, respectively. The formation enthalpies for K_2TiH_6 and Ca_2TiH_6 were determined to be −0.0750 eV/atom and −0.3717 eV/atom, respectively. The formation enthalpy (ΔH) was approximated from the total energy difference obtained via DFT, assuming $\Delta H \approx \Delta E$ since the PV contribution is negligible for solids at low pressure. The calculated energy difference was normalized by the total number of atoms in the formula unit, and thus reported in eV/atom. The negative enthalpy of formation signifies that the estimated materials can be produced experimentally and are thermodynamically stable [23,24].

3.2. Electronic properties

In modern materials science and quantum chemistry, understanding the physical and chemical properties of a material depends on accurately modeling its electronic structure at the atomic level. Electronic structure calculations play a critical role in determining energy bands, bond characteristics, and magnetic properties, particularly in solid-state systems. Fig. 2 shows the electronic band structure graphs of K_2TiH_6 and Ca_2TiH_6 compounds drawn along high symmetry axes under pressures of 0, 5, 10, 15, and 20 GPa. The Fermi energy level (EF) is set to 0 eV. Below the Fermi energy level lies the valence band (VB). On the other hand, above the Fermi energy level are the conduction bands (CB). The Fermi energy level is indicated by a dashed line. If the valence band and conduction band intersect at the Fermi energy level, the material exhibits metallic properties. If there is a band gap around the Fermi energy level between the valence band and the conduction band, the material exhibits semiconducting or insulating properties depending on the value of the band gap.

The band structures shown on the left side of Fig. 2 represent the electronic band structure of the K_2TiH_6 compound obtained under different hydrostatic pressure values (0, 5, 10, 15, and 20 GPa). The results obtained reveal that the K_2TiH_6 compound exhibits a non-magnetic character across all pressure values. Band structure analyses reveal the presence of a distinct band gap between the valence band (VB) and the conduction band (CB). According to calculations performed at zero pressure (0 GPa), the K_2TiH_6 compound has a direct band gap. There is a band gap of approximately 1.8 eV between the maximum of the valence band and the minimum of the conduction band, indicating that the material exhibits semiconducting properties. The presence of a band gap indicates that electron transitions will only occur at the appropriate energy gain and that electrical conductivity will be limited. As pressure increased (5, 10, and 15 GPa), although some minor changes were observed in the band structure, the overall band gap remained unchanged. This indicates that the electronic structure of the K_2TiH_6 compound is highly stable under pressure and does not undergo a structural phase transition or acquire metallic character. Since no spin separation was observed between the valence and conduction bands, it was confirmed that the system does not exhibit magnetic properties. Even after applying high pressure (20 GPa), the band structure of the K_2TiH_6 compound retained a distinct band gap, and it was determined that the material maintained its semiconducting character. This indicates that the K_2TiH_6 compound maintains an electronically and structurally stable structure under high pressure and does not acquire magnetic properties. Additionally, the preservation of the distance between the upper valence band and the lower conduction band in the band structure suggests that this compound could be a suitable candidate for electronic devices and semiconductor technologies.

The band structures shown in the right part of Fig. 2 illustrate the electronic behavior and magnetic properties of the Ca_2TiH_6 compound under pressure. Due to the magnetic character of the Ca_2TiH_6 compound, the band structures were calculated separately for the spin-up and spin-down states. This is an important indicator that the material exhibits ferromagnetic properties. At zero pressure, the Ca_2TiH_6

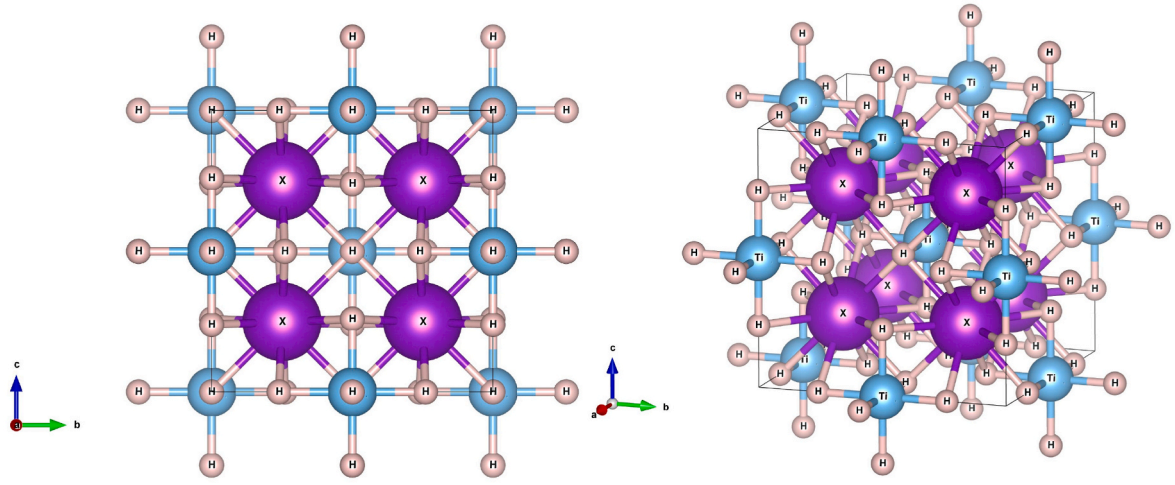

Fig. 1. Crystal structures of the X2TiH6 compound obtained from different directions.

Table 1
The lattice parameter (a_0), volume (V), and density (ρ) values obtained for K_2TiH_6 and Ca_2TiH_6 compounds under different hydrostatic pressure values (0, 5, 10, 15, and 20 GPa).

Materials	K_2TiH_6			Ca_2TiH_6		
P(GPa)	$\mathbf{a_0}$ (Å)	$\mathbf{V}(Å^3)$	$\boldsymbol{\rho}$ $(\mathbf{g}/cm\mathbf{3})$	$\mathbf{a_0}$ (Å)	$\mathbf{V}(Å^3)$	$\boldsymbol{\rho}$ $(\mathbf{g}/cm\mathbf{3})$
0	8.5535	625.7946	1.402223	7.4698	416.7934	2.136594
5	7.8625	486.059	1.805344	7.2289	377.7635	2.357343
10	7.4568	414.6317	2.116345	7.0556	351.2399	2.535356
15	7.2804	385.8893	2.273977	6.9145	330.5801	2.693804
20	7.0984	357.6766	2.453343	6.7974	314.0737	2.835380

compound shows a distinct difference between the spin-up and spin-down band structures. While a semiconducting character is observed in the spin-up channel, conductivity properties are more dominant in the spin-down channel. This situation reveals that the material exhibits half-metallic behavior. In half-metallic materials, the presence of conductivity in one spin channel and a band gap in the other spin channel is of great importance for spintronic applications. As pressure increases (5, 10, and 15 GPa), some changes are observed in the band structure, but the difference between the spin-up and spin-down band structures is preserved. These results show that the magnetic character of the Ca_2TiH_6 compound is quite stable against pressure and maintains its ferromagnetic properties. Additionally, the continued spin separation in the band structure indicates that the material's spin polarization is preserved and its spin filtering property persists. Even after applying high pressure (20 GPa), it was observed that the Ca_2TiH_6 compound retains its magnetic properties. The difference between the spin-up and spin-down band structures persists, and it is understood that it maintains its metallic character properties. This suggests that the Ca_2TiH_6 compound could be a suitable material candidate for spintronic applications even under high pressure.

In Fig. 3(a), when the PDOS graph obtained at 0 GPa pressure is examined, it is seen that the K_2TiH_6 compound exhibits semiconductor properties. There is a distinct band gap between the valence band maximum and the conduction band minimum. In the valence band, the dominant contribution of H-1s and Ti-3d orbitals in the energy range between −5 eV and 0 eV is noteworthy. This indicates that Ti–H interactions play an important role in the chemical bond structure of the compound. The conduction band, on the other hand, is primarily composed of Ti-3d orbitals. The contribution of K atoms is quite low, suggesting that K atoms mainly contribute to structural stability and do not significantly affect the bond structure. When the pressure is increased to 5 GPa, the fundamental characteristics of the band structure are preserved. The band gap persists, and Ti-3d and H-1s orbitals remain dominant in the valence band. However, slight shifts and compressions in energy levels are observed. This indicates that the external forces exerted by pressure on the structure reduce interatomic distances, strengthen interactions, and alter energy levels. When 10 GPa pressure is reached, a certain narrowing in the bandwidth is observed. The valence band levels have approached the Fermi level to a certain extent. The conduction band continues to be Ti-3d in character. Even at this pressure, the compound continues to exhibit semiconducting behavior, with no significant closing of the band gap. Although the increase in pressure increases structural compaction, no transformation that would convert the electronic structure to a metallic state has been observed. At 15 GPa pressure, the dominance of Ti-3d and H-1s orbitals in the valence and conduction bands continues. No significant changes in the band structure are observed, and the band gap remains intact. It is noteworthy that the compression of energy levels has increased slightly and the width of the bands has narrowed. Even at this pressure value, the K_2TiH_6 compound retains its semiconducting properties. At 20 GPa pressure, the compound also maintains its semiconducting character. There is no orbital density at the Fermi level. The band gap is still present, and the dominance of Ti-3d orbitals in the conduction band is maintained. Although compression in the band structure is observed with increasing pressure, no metallic phase transition is observed. This indicates that the electronic structure of the K_2TiH_6 compound is highly stable under high pressure.

In Fig. 3(b), when the PDOS analysis of the Ca_2TiH_6 compound under 0 GPa pressure is examined, it is observed that the compound exhibits magnetic character and there is a difference between the spin-up and spin-down channels. There is a particularly strong contribution from Ti-3d orbitals around the Fermi level. The valence band is located between −6 eV and 0 eV, where the effects of H-1s and Ti-3d orbitals are dominant. Just below the Fermi level, the spin separation of Ti-3d orbitals is observed. When the pressure is increased to 5 GPa, there is no significant change in the structure of the valence band and conduction band. The spin separation at the Fermi level is preserved. The contribution of the Ti-3d orbitals is evident in both the spin-up and spin-down channels. The valence bandwidth has narrowed slightly. The contribution of the Ca orbitals is quite low in both the valence and conduction bands. Under 10 GPa pressure, it is observed that the compression in the band structure increases, and the energy levels approach the Fermi level slightly more. However, there is no significant closing in the band gap. Spin separation continues, and magnetic properties are preserved. It is clearly seen that Ti-3d orbitals are dominant in both the valence band and the conduction band. As pressure increases, the contribution of Ti-3d orbitals in the valence band becomes even more pronounced. Spin separation is still present. The density at the Fermi level originates from Ti-3d orbitals. This indicates that the Ca_2TiH_6 compound retains its magnetic properties despite pressure. The H-1s contribution in the valence band continues to be clear. Even when the pressure reaches 20 GPa, the compound still exhibits magnetic properties. The difference between the spin-up and spin-down channels continues. The dominance of Ti-3d orbitals around the Fermi level continues to increase. No significant closing of the band gap is observed. At this pressure level, it is seen that the Ca_2TiH_6 compound does not transition to a metallic state, but rather that the compression of energy levels increases. Additionally, the hydrogen storage behavior of X_2TiH_6 compounds is strongly correlated with their electronic structure. The DOS analysis reveals that Ti–3d and H-1s orbitals dominate the bonding states, indicating that hydrogen is stabilized through Ti–H hybridization within the $[TiH_6]^{2-}$ octahedra. In K_2TiH_6, the semiconducting band gap and weaker Ti–H bonding lead to a lower desorption temperature. In contrast, Ca_2TiH_6 exhibits spin-polarized metallic character, stronger Ti–H interactions, and correspondingly higher hydrogen desorption temperatures. Therefore, the electronic configuration not only determines the stability of the hydrides but also directly controls their hydrogen release behavior.

3.3. Thermodynamic properties

The hydrogen storage behavior of X_2TiH_6 compounds is closely linked to their thermodynamic response under varying temperature and pressure. The increase in vibrational energy and entropy with temperature facilitates the breaking of Ti–H bonds and promotes H_2 desorption, while the decrease in free energy at elevated temperatures indicates reduced hydride stability. Conversely, the application of pressure enhances structural rigidity, decreases entropy, and suppresses hydrogen release. Therefore, thermodynamic properties govern the balance

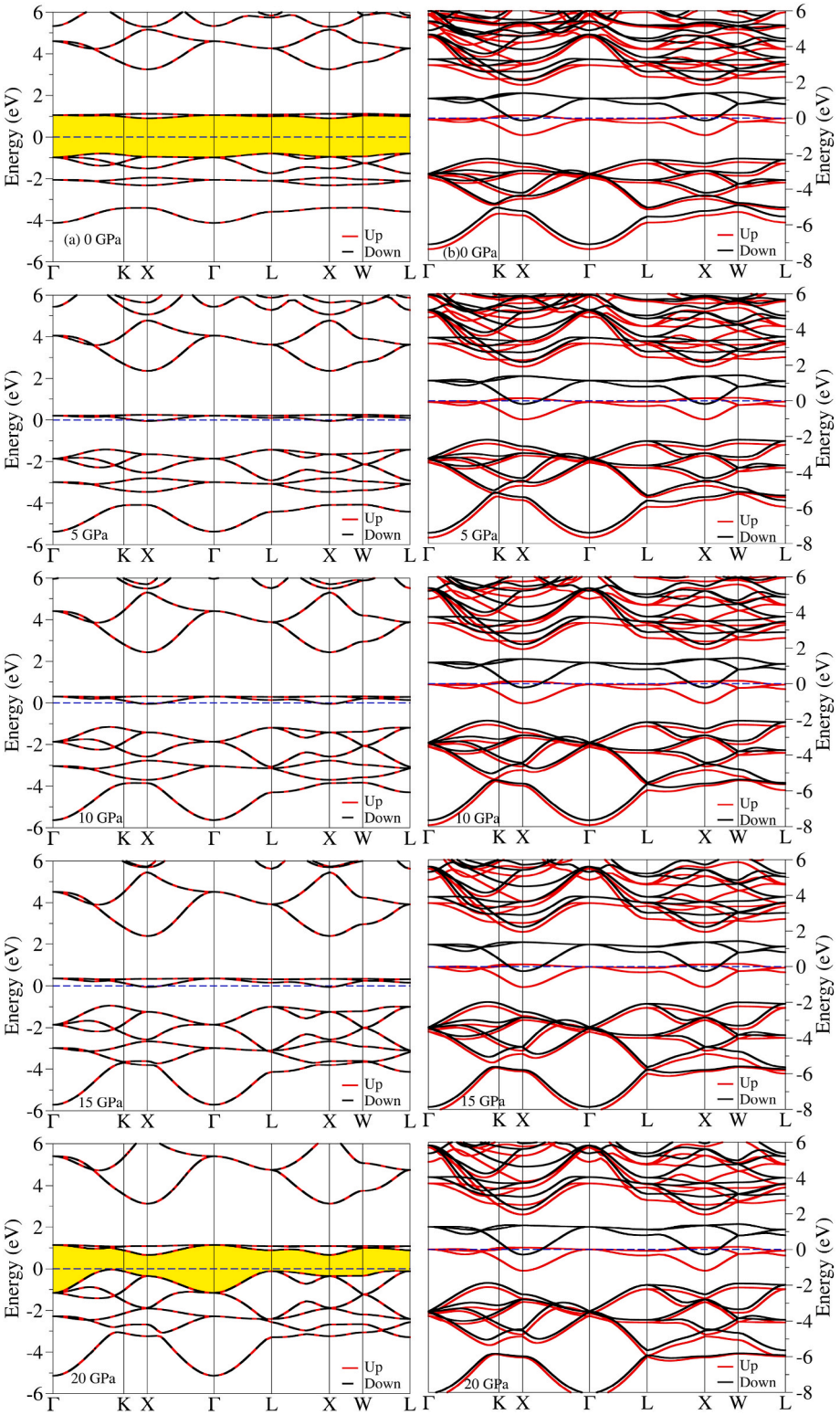

Fig. 2. Electronic band structure of K_2TiH_6 (left) and Ca_2TiH_6 (right) compounds obtained under different hydrostatic pressure values (0, 5, 10, 15, and 20 GPa).

between stability and hydrogen release, with K_2TiH_6 exhibiting a lower desorption temperature due to its weaker Ti–H interactions, and Ca_2TiH_6 displaying higher thermal stability and correspondingly higher desorption temperatures. Fig. 4 shows the thermal properties that describe the thermal response of a material. Vibrational energy (a), vibrational free energy (b), entropy, and heat capacity as a function of temperature were examined in detail for the K_2TiH_6 compound at pressures of 0, 5, 10, 15, and 20 GPa.

Fig. 4 (a) shows the change in vibrational energy of the K_2TiH_6 compound with temperature under different pressure conditions between 0 and 20 GPa. Upon examining the graph, it is observed that vibrational energy increases regularly with temperature. It is seen that the increase in pressure has a significant effect on the energy values at low temperatures (0–200 K), but as the temperature increases ($T > 300$

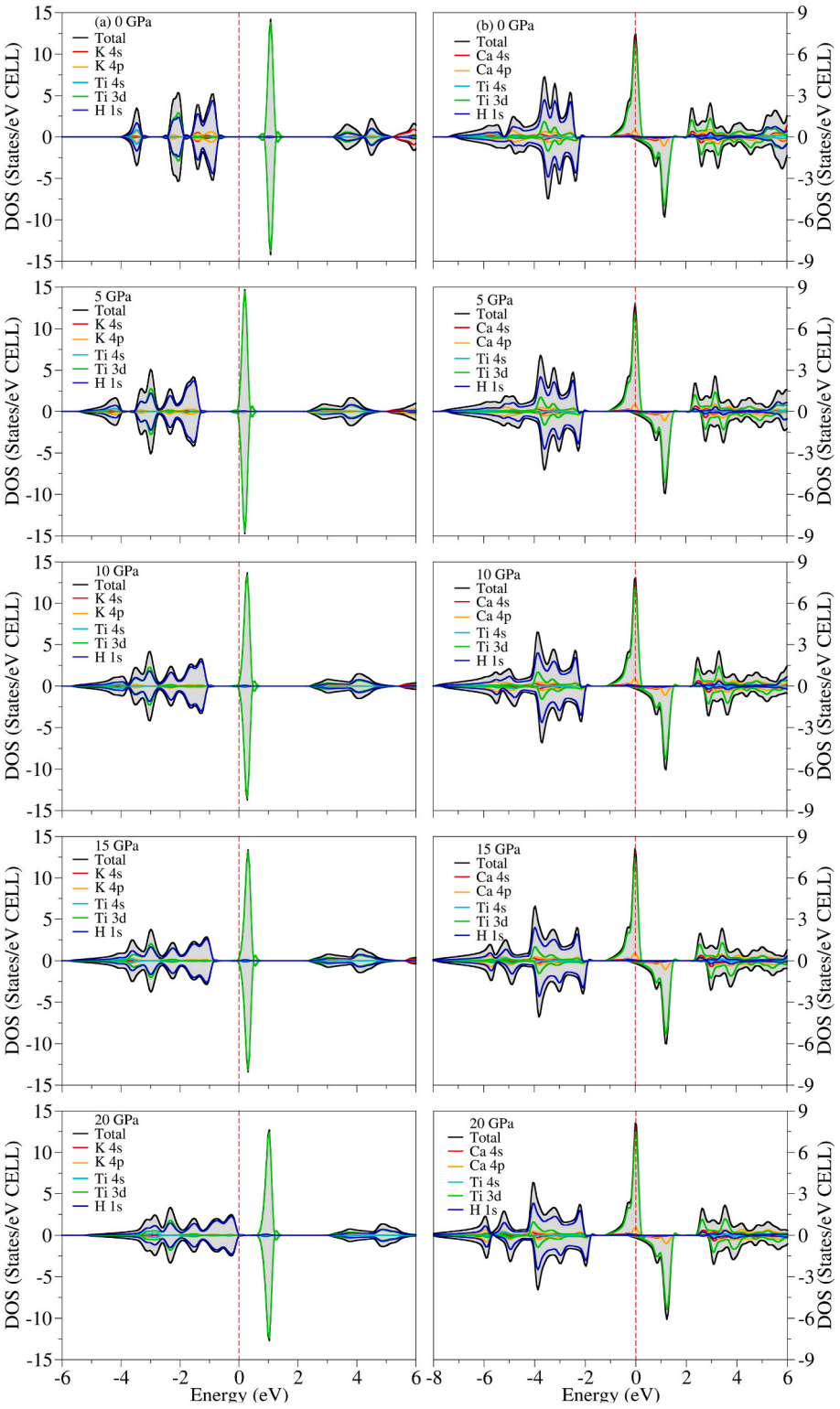

Fig. 3. Total and partial state density graphs obtained for K_2TiH_6 (left) and Ca_2TiH_6 (right) compounds under different hydrostatic pressure values (0, 5, 10, 15, and 20 GPa).

K), these differences decrease. Under high pressure, the energy of the system's vibrational modes increases, which can be attributed to the strengthening of interatomic interactions. However, at high temperatures, all pressure values converge, and the system's energy reaches approximately 180 kJ/mol. This indicates that the temperature effect suppresses the high-pressure effect. Fig. 4 (b) shows the change in the vibrational free energy of K_2TiH_6 with temperature and its sensitivity to pressure. The free energy decreases monotonically as the temperature increases. The free energy curves follow a similar trend at all pressure values, reaching the lowest value at 0 GPa. This indicates that the system is not more stable at low pressure but rather exhibits a lower (negative) free energy under high pressure and thus a more stable structure. The effect of pressure becomes more pronounced at temperatures above 600 K. Fig. 4(c) shows the change in entropy of the K_2TiH_6 compound with

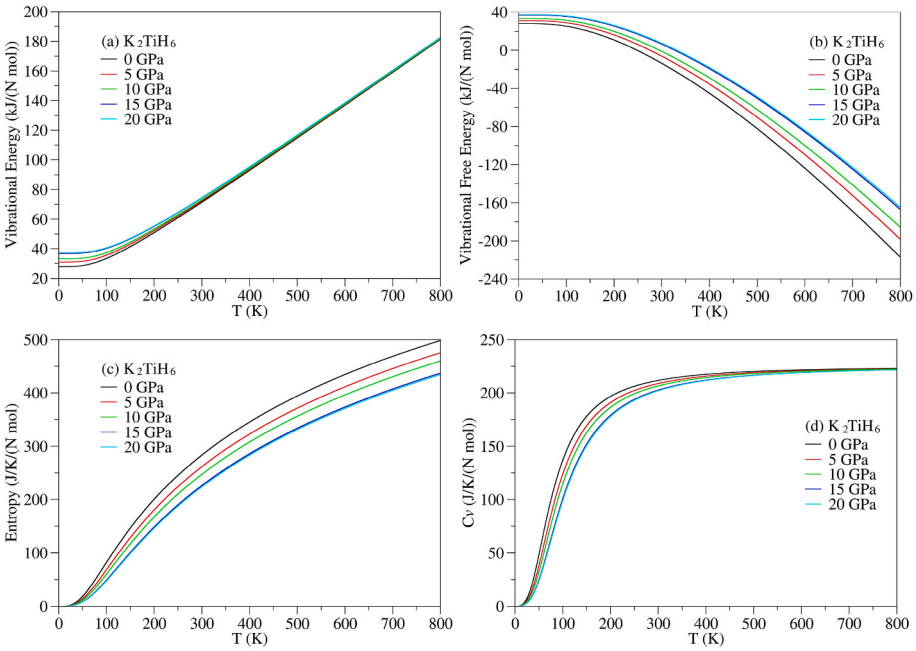

Fig. 4. Temperature-dependent change in the thermal properties of the K_2TiH_6 compound obtained under different hydrostatic pressure values (0, 5, 10, 15, and 20 GPa).

temperature. Entropy increases continuously with temperature, which is a thermodynamically expected situation. At high temperatures, the disorder of atoms increases, leading to higher entropy values. Interestingly, it is observed that entropy values decrease with increasing pressure. This situation shows that pressure reduces the disorder of the system by limiting the mobility of atoms, thereby decreasing entropy. For example, the entropy value of approximately 480 J/K·mol at 800 K and 0 GPa decreases to approximately 420 J/K·mol at 20 GPa. Fig. 4(d) shows the relationship between heat capacity (Cv) and temperature at constant volume. The Cv value exhibits a rapid increase at low temperatures, then reaches saturation at high temperatures and stabilizes at approximately 210 J/K·mol. This behavior is consistent with the Debye model, indicating that phonon contributions dominate at low temperatures and that Cv reaches a constant value at high temperatures due to the excitation of all phonon modes. Additionally, it is observed that the Cv value decreases slightly as pressure increases. This may be attributed to the restriction of atomic vibrational modes by pressure.

Furthermore, Fig. 5 shows the thermal properties of the Ca_2TiH_6 compound under pressures of 0, 5, 10, 15, and 20 GPa.

In this study, the basic thermodynamic properties of the Ca_2TiH_6 compound were examined in detail in the pressure range of 0–20 GPa and the temperature range of 0–800 K. The evaluations made on the

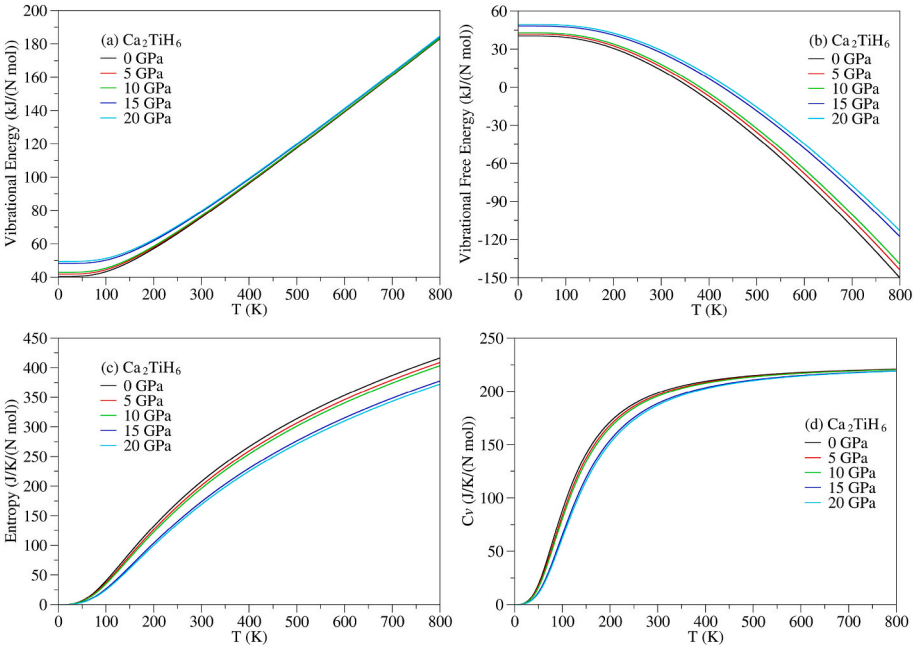

Fig. 5. Temperature-dependent change in the thermal properties of the Ca_2TiH_6 compound obtained under different hydrostatic pressure values (0, 5, 10, 15, and 20 GPa).

obtained graphs are presented below. As seen in Fig. 5(a), the vibrational energy of the Ca_2TiH_6 compound increases monotonically with temperature. This increase can be attributed to the increase in the vibration amplitudes of the atoms as the temperature rises. The effect of pressure is more pronounced at low temperatures. In particular, there is a noticeable increase in vibration energy as pressure increases between 0 and 100 K. The highest values of vibrational energy are observed at 15 GPa and 20 GPa pressure applications. This indicates that under high pressure, interatomic bonds stiffen, and vibrational modes gain energy. However, at high temperatures (T > 500 K), all pressure curves converge, and the pressure effect loses its distinctiveness. The results in Fig. 5 (b) clearly show that the free energy of vibration decreases as the temperature increases. This is to be expected, since free energy includes both internal energy and entropic contribution. At low temperatures, it is observed that free energy increases as pressure increases. This result indicates that the stability of the system increases under high pressure and that more positive free energy values are reached. At high temperatures, all pressure curves approach each other, reaching values around −150 kJ/mol. This situation demonstrates the dominant effect of temperature on free energy.

Fig. 5 (c) shows a significant increase in entropy with temperature. Since entropy is an indicator of the disorder and freedom of movement of atoms, its increase with temperature is an expected behavior. The effect of pressure is in the opposite direction. A decrease in entropy values is observed with increasing pressure. This decrease becomes more pronounced in the 0–200 K range. It is understood that under high pressure, the mobility of atoms is restricted and the order within the structure increases. The highest entropy values are obtained at 0 GPa pressure, while the lowest entropy values are observed at 20 GPa pressure. Fig. 5 (d) shows the change in specific heat capacity (C_v) values with temperature at constant volume. C_v values increase rapidly at low temperatures, reaching a saturation point at approximately 300 K. After this temperature, C_v values remain constant regardless of pressure. In the low-temperature region, small decreases in C_v values were observed as pressure increased. This can be explained by the restriction of phonon modes under high pressure and the system becoming more rigid. However, at high temperatures, the pressure effect is minimized due to reaching the classical Dulong-Petit limit.

3.4. Elastic properties

Elastic properties are considered a critical parameter for determining the mechanical stability of a crystal structure and its resistance behavior against external factors. Elastic constants (C_{11}, C_{12}, C_{44}), bulk modulus (B), shear modulus (G), Young's modulus (E), Poisson's ratio (ν), and the B/G ratio are elastic parameters used to characterize the hardness, ductility, rigidity, and mechanical stability of materials. In this context, the elastic properties of K_2TiH_6 and Ca_2TiH_6 compounds under different pressure values (0–20 GPa) were systematically investigated, and the results are presented in Table 2. The mechanical stability of crystalline materials under applied pressure can be evaluated using the Born stability criteria, which determine whether a crystal structure can remain mechanically stable against small deformations. For cubic crystal systems, these criteria require that the elastic constants satisfy the conditions [25].

$$(C_{11} - C_{12}) > 0, (C_{11} + 2C_{12}) > 0, C_{11} > 0, C_{44} > 0, C_{12} < B < C_{11} \quad (2)$$

These conditions ensure that the structure can provide a positive stress-strain response under applied stress and can resist shear and volumetric deformations, indicating its mechanical stability under external influences. In the present study, the calculated elastic constants for K_2TiH_6 and Ca_2TiH_6 compounds under various pressure values were found to satisfy the Born stability criteria across the entire pressure range of 0–20 GPa. This confirms that both compounds maintain their mechanical stability under high-pressure conditions, supporting the reliability of the elastic property calculations presented in this work.

The elastic constants obtained for the K_2TiH_6 compound show a marked increase with increasing pressure. The low C_{11} and C_{44} values obtained at 0 GPa indicate that the structure has low mechanical stability and a brittle character. However, it has been observed that the elastic constants exhibit a non-linear but continuous increase trend as pressure increases. The rapid increase in C_{11} and C_{44} constants observed after 10 GPa indicates that the structure begins to gain rigidity. The bulk modulus (B), shear modulus (G), and Young's modulus (E) values also increased regularly with increasing pressure, indicating that the structure's compressibility decreased and its strength increased. Additionally, the increase in the Poisson's ratio (υ) value indicates that the structure's flexibility increased in response to pressure and that it tended to transition from a brittle character to a ductile character. It is known that materials exhibit ductile behavior when the B/G ratio exceeds 1.75. In this context, it was observed that brittle properties dominate at low pressures in the K_2TiH_6 compound, while ductile properties come to the fore at pressures of 10 GPa and above. At 20 GPa pressure, the K_2TiH_6 compound was observed to transform into a rigid, durable, and ductile structure by reaching maximum elastic parameters.

The Ca_2TiH_6 compound is seen to have superior mechanical properties compared to the K_2TiH_6 compound in terms of elastic parameters from the outset. Even at 0 GPa pressure, the high C_{11} and C_{44} constants indicate that the structure is highly rigid and durable. This can be attributed to the contribution of the Ca element to the crystal structure. The increase in elastic constants with increasing pressure is regular and distinct. The shear modulus and bulk modulus values indicate that the structure has reduced compressibility and high shear strength. The Young's modulus values confirm that the Ca_2TiH_6 compound has excellent flexibility and durability, especially under high pressure conditions. The high Poisson's ratio (ν) value indicates that the structure is ductile rather than brittle. Additionally, the B/G ratio remained above 1.75 across all pressure ranges, demonstrating that the Ca_2TiH_6 compound can maintain its ductility even under high-pressure conditions. As pressure increased, the compound exhibited high mechanical stability, low compressibility, and high elastic strength.

Table 2
Elastic constants (Cij), bulk modulus (GPa), Young's modulus (GPa), shear modulus (GPa), B/G ratio, and Poisson's ratio (υ) values obtained for K_2TiH_6 and Ca_2TiH_6 compounds under different hydrostatic pressure values (0, 5, 10, 15, and 20 GPa).

Materials	Pressure	C_{11}	C_{12}	C_{44}	B	E	G	B/G	υ
	0	23.69	5.795	10.15	11.76	22.73	9.65	1.21	0.178
	5	44.79	23.59	13.99	30.65	33.06	12.51	2.45	0.32
K_2TiH_6	10	60.47	29.75	14.9	39.99	40.19	15.08	2.65	0.33
	15	77.57	51.85	24.88	60.42	51.8	19.09	3.16	0.36
	20	89.01	66.38	29.73	73.92	55.45	20.18	3.66	0.37
	0	72.34	29.37	23.96	43.69	58.57	22.94	1.90	0.28
	5	88.49	45.35	27.91	59.73	66.22	25.18	2.37	0.32
Ca_2TiH_6	10	103.38	60.97	31.79	75.11	72.39	27.03	2.77	0.34
	15	122.70	66.72	40.66	85.38	92.39	35.01	2.43	0.32
	20	138.78	82.31	45.01	101.14	99.72	37.33	2.70	0.34

3.5. Hydrogen storage properties

The gravimetric storage capacity ($C_{wt\%}$) and the desorption temperature (T_{des}) of hydrides, or potential hydrogen storage materials, are two essential factors. $C_{wt\%}$ is the quantity of hydrogen that can be kept per unit weight of the material, whereas T_{des} signifies the temperature at which hydrogen can be liberated from the material. These characteristics are essential in assessing the efficacy and feasibility of a hydride as a hydrogen storage medium. Optimal features for a hydride material include a high $C_{wt\%}$ and a low T_{des}, facilitating increased hydrogen storage and release at controllable temperatures. The gravimetric storage capacity is determined using Equation (3).

$$C_{wt\%} = \left(\frac{\left(\frac{H}{M}\right) M_H}{M_{Host} + \left(\frac{H}{M}\right) M_H} x\,100 \right)\% \tag{3}$$

The molecular weight of hydrogen is denoted by MH, the molecular weight of the host material is denoted by M_{Host}, and the hydrogen-to-metal ratio is represented by the H/M symbol. The predicted gravimetric capacities are 4.58 wt% for K_2TiH_6, and 4.51 wt% for Ca_2TiH_6. These values indicate that both compounds possess good hydrogen storage capacity and practical applicability. In addition to gravimetric storage capacity, desorption temperature is another critical parameter for hydrogen storage materials. The temperature can be approximated with the standard Gibbs formula, as demonstrated in the equations below:

$$\Delta G = \Delta H - T_{des}\Delta S \tag{4}$$

Here, ΔH represents the enthalpy of the reaction and is computed as follows. $\Delta H = \Sigma_{products}E - \Sigma_{reactants}E$. Under standard pressure and temperature circumstances, where $\Delta G = 0$, T_{des} can be determined using the equation:

$$T_{des} = \frac{\Delta S}{\Delta H} \tag{5}$$

The desorption temperatures for K_2TiH_6, and Ca_2TiH_6 are 55.40 K and 274.40 K, respectively. Regarding desorption temperatures, a notably low value of 55.40 K was obtained for K_2TiH_6, while a higher value of 274.40 K was calculated for Ca_2TiH_6. The low desorption temperature suggests that K_2TiH_6 can release hydrogen at lower temperatures, whereas Ca_2TiH_6 can release hydrogen at higher temperatures. Additionally, the hydrogen storage mechanism in X_2TiH_6 compounds arises from the Ti-centered $[TiH_6]^{2-}$ octahedral units, in which hydrogen atoms form strong Ti–H interactions. The electropositive K^+/Ca^{2+} cations provide charge balance and structural stabilization to the framework. During desorption, thermal excitation breaks the Ti–H bonds, and hydrogen atoms recombine to form H_2 molecules. The different desorption temperatures of K_2TiH_6 and Ca_2TiH_6 can be directly attributed to the relative Ti–H bond strengths, with Ca_2TiH_6 exhibiting stronger Ti–H interactions and therefore requiring higher thermal energy for hydrogen release. These results demonstrate that K_2TiH_6 is suitable for hydrogen release in low-temperature applications, while Ca_2TiH_6 is a promising candidate for systems requiring hydrogen release at higher temperatures.

3.6. Phonon properties

Phonon calculations of materials, particularly in solid-state physics, are conducted to comprehend and simulate the thermal and kinetic properties of substances. Phonons are quasi-particles arising from atomic vibrations within a crystal lattice, and these vibrations influence numerous physical properties of materials. Phonons consist of two components: acoustic and optical. Acoustic phonons denote low-energy vibrations characterized by the coherent oscillation of atoms in a wave-like fashion, akin to sound waves. These phonons predominate in thermal conduction within solids. Optical phonons occur in crystals containing several atoms per unit cell, when the atoms oscillate out of phase with one another. These phonons are crucial in optical and infrared absorption mechanisms. Figs. 6 and 7 present the distribution of acoustic and optical modes along the axis of high symmetry for the K2TiH6 and Ca2TiH6 compounds at 0 GPa pressure, respectively.

Given that there are N = 9 atoms in the unit cell of this structure, it possesses a total of 3 N, or 27 modes. Of these modes, 3 are acoustic, while the remaining 24 are visual. Examining phonon modes can assist in ascertaining the stability of a crystal structure. The presence of phantom (negative frequency) phonons in a material signifies dynamic instability, suggesting a potential transformation into an alternative structure. If all phonon frequencies are positive, as indicated in this study, the structure is dynamically stable.

4. Conclusion

In this study, the structural, electronic, mechanical, thermodynamic, vibrational, and hydrogen storage behaviors of K_2TiH_6 and Ca_2TiH_6 complex hydride compounds under high pressure were analyzed in detail using first-principles calculations based on density functional theory (DFT). Electronic band structure analyses revealed that the K_2TiH_6compound exhibits a non-magnetic semiconductor structure at all pressure values. On the other hand, the Ca_2TiH_6 compound exhibits magnetic character, creating a distinction between spin-up and spin-down channels. This spin distinction indicates that Ca_2TiH_6 exhibits metallic properties. In terms of thermodynamic properties, the parameters of both compounds, such as vibrational energy, free energy, entropy, and heat capacity, change in a temperature- and pressure-sensitive manner. In particular, free energy reaches minimum values at low temperatures and high pressures, indicating an increase in the thermodynamic stability of the system. The increase in entropy values at high temperatures and their decrease with pressure indicate that atomic-level disorder and compression effects shape system behavior as expected. C_v (heat capacity at constant volume) values exhibited behavior consistent with the Debye model and showed stability with small changes depending on pressure. From a mechanical perspective, both compounds met the Born mechanical stability criteria under the applied pressures. K_2TiH_6 exhibits brittleness at low pressures but transitions to ductile behavior at pressures above 10 GPa. This is clearly supported by the B/G ratio and Poisson's ratio. The Ca_2TiH_6 compound has maintained its ductility and elasticity properties across all pressure ranges with $B/G > 1.75$ and a high Poisson's ratio. The absence of imaginary frequencies in all phonon branches indicates that both K_2TiH_6 and Ca_2TiH_6 are dynamically stable at 0 GPa.

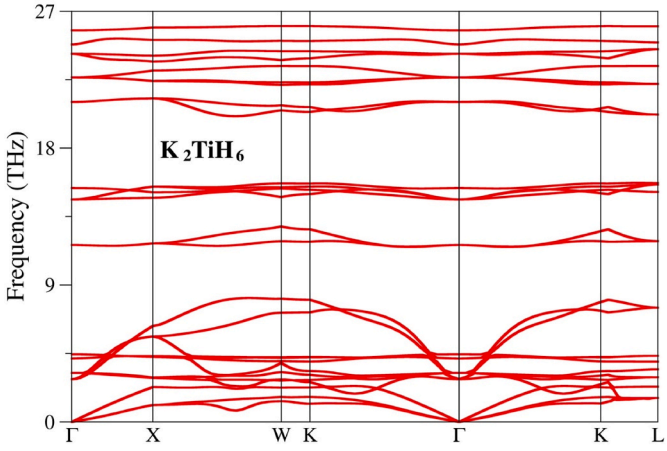

Fig. 6. Phonon dispersion curves of K_2TiH_6 along high-symmetry directions.

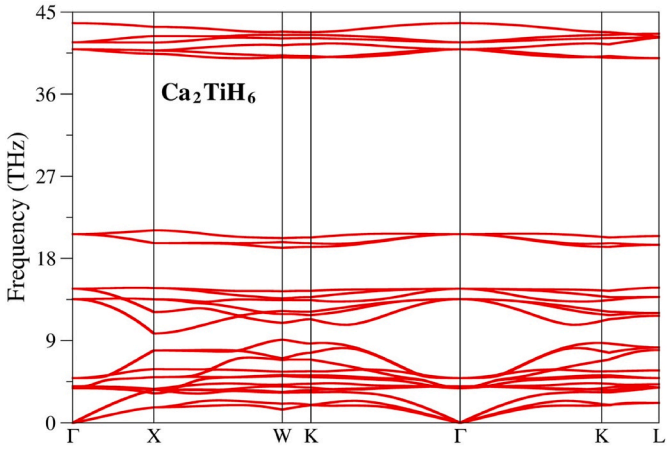

Fig. 7. Phonon dispersion curves of Ca_2TiH_6 along high-symmetry directions.

CRediT authorship contribution statement

Salih Ermiş: Writing – original draft, Software. **Ahmet İyigör:** Writing – review & editing, Writing – original draft, Methodology. **Cihan Kürkçü:** Writing – review & editing, Writing – original draft, Resources, Methodology, Funding acquisition.

Declaration of generative AI and AI-assisted technologies in the writing process

During the preparation of this work, the author(s) used an artificial intelligence tool to improve the language and readability of the study. After using this tool/service, the author(s) reviewed and edited the content as needed and take(s) full responsibility for the content of the publication.

Declaration of competing interest

The authors declare that they have no known competing financial interests or personal relationships that could have appeared to influence the work reported in this paper.

Acknowledgment

This study was supported by the Kırşehir Ahi Evran University under Scientific Research Project No: TBY.A1.24.001.

References

[1] Örnek O, Al S, İyigor A, Lafci S. Electronic and elastic properties cubic of LiBH4 and Li (BH) 3 as host materials for hydrogen storage. Eur Phys J B 2024;97:9.
[2] Noor WB, Amin T. Towards sustainable energy: a comprehensive review on hydrogen integration in renewable energy systems. Future Energy 2024;3:1–17.
[3] Zafar M, Iqbal T, Fatima S, Sanaullah Q, Aman S. Carbon nanotubes for production and storage of hydrogen: challenges and development. Chem Pap 2022:1–17.
[4] Ni M. An overview of hydrogen storage technologies. Energy Explor Exploit 2006; 24:197–209.
[5] Turner JA. Sustainable hydrogen production. Science 2004;305:972–4.
[6] Schlapbach L, Züttel A. Hydrogen-storage materials for mobile applications. nature 2001;414:353–8.
[7] Yamçıçıer Ç, Kürkçü C. Ab initio study of the structural, mechanical, optoelectronic and thermo-physical properties of XGaH5 (X= Ba, Ca, and Mg) compounds for hydrogen storage applications. Int J Hydrogen Energy 2024;81:391–404.
[8] Yamçıçıer Ç, Kürkçü C. Investigation of structural, electronic, elastic, vibrational, thermodynamic, and optical properties of Mg2NiH4 and Mg2RuH4 compounds used in hydrogen storage. J Energy Storage 2024;84:110883.
[9] Züttel A. Materials for hydrogen storage. Mater Today 2003;6:24–33.
[10] Sakintuna B, Lamari-Darkrim F, Hirscher M. Metal hydride materials for solid hydrogen storage: a review. Int J Hydrogen Energy 2007;32:1121–40.
[11] Orimo S-i, Nakamori Y, Eliseo JR, Züttel A, Jensen CM. Complex hydrides for hydrogen storage. Chem Rev 2007;107:4111–32.
[12] Zurek E. Hydrides of the alkali metals and alkaline earth metals under pressure. Comments Mod Chem 2017;37:78–98.
[13] He T, Cao H, Chen P. Complex hydrides for energy storage, conversion, and utilization. Adv Mater 2019;31:1902757.
[14] Dematteis EM, Amdisen MB, Autrey T, Barale J, Bowden ME, Buckley CE, et al. Hydrogen storage in complex hydrides: past activities and new trends. Progress in Energy 2022;4:032009.
[15] Chen B, Qiu F, Xia L, Xu L, Jin J, Gou G. In situ ultrasonic characterization of hydrogen damage evolution in X80 pipeline steel. Materials 2024;17:5891.
[16] Wang H, Hou Y, He Y, Wen C, Giron-Palomares B, Duan Y, et al. A Physical-constrained decomposition method of infrared thermography: pseudo restored heat flux approach based on ensemble Bayesian variance tensor fraction. IEEE Trans Ind Inf 2023;20:3413–24.
[17] Perdew JP, Burke K, Ernzerhof M. Generalized gradient approximation made simple. Phys Rev Lett 1996;77:3865.
[18] Giannozzi P, Baroni S, Bonini N, Calandra M, Car R, Cavazzoni C, et al. QUANTUM ESPRESSO: a modular and open-source software project for quantumsimulations of materials. J Phys Condens Matter 2009;21:395502.
[19] Giannozzi P, Andreussi O, Brumme T, Bunau O, Nardelli MB, Calandra M, et al. Advanced capabilities for materials modelling with quantum ESPRESSO. J Phys Condens Matter 2017;29:465901.
[20] Monkhorst HJ, Pack JD. Special points for Brillouin-zone integrations. Phys Rev B 1976;13:5188.
[21] Dal Corso A. Pseudopotentials periodic table: from H to Pu. Comput Mater Sci 2014;95:337–50.
[22] Yamçıçıer Ç, Kürkçü C. Structural, elastic, optic, electronic, phonon, thermodynamic, and hydrogen storage properties of bialkali alanates M2LiAlH6 (M= Na, K). Int J Hydrogen Energy 2025;135:440–56.
[23] Surucu G, Candan A, Gencer A, Isik M. First-principle investigation for the hydrogen storage properties of NaXH3 (X= Mn, Fe, Co) perovskite type hydrides. Int J Hydrogen Energy 2019;44:30218–25.
[24] Soykan C, Kürkçü C. First-principles calculations to investigate structural, electronic, mechanical, optical, vibrational, thermal properties, and hydrogen storage capabilities of Rb2SnH4 for hydrogen storage applications. J Phys Chem Solid 2025:112618.
[25] Born M. On the stability of crystal lattices. I. In: Mathematical proceedings of the Cambridge philosophical society. Cambridge University Press; 1940. p. 160–72.